J. Phys. C: Solid State Phys. **18** (1985) 3001–3010. Printed in Great Britain

# Thermal conductivity of tin-doped bismuth between 50 mK and 7 K

C Uher†, J Heremans‡‖, J-P Issi‡, A M de Goër§ and M Locatelli§

† Physics Department, University of Michigan, Ann Arbor, Michigan 48109, USA
‡ Université Catholique de Louvain, Laboratoire de Physico-Chimie et de Physique de l'Etat Solide, Place Croix-du-sud 1, B-1348 Louvain-la-Neuve, Belgium
§ Service des Basses Temperatures, Laboratoire de Cryophysique, Centre d'Etudes Nucléaires de Grenoble, 85X, 38041, Grenoble Cedex, France

Received 29 May 1984, in final form 28 November 1984

**Abstract.** We report on the thermal conductivity of tin-doped bismuth between 50 mK and 27 K. A quantitative interpretation of the data is presented. At the lowest temperatures the electronic thermal conductivity dominates, but above 0.1 K lattice waves carry most of the heat. Below 1 K phonons are scattered mostly by crystal boundaries, while near the dielectric maximum point defects are important. Their scattering rate is directly proportional to the atomic concentration of the tin impurity.

## 1. Introduction

Bismuth is a typical semimetal with a very small free carrier density. The thermal conductivity of Bi, like its other transport properties, has been the subject of numerous studies over the past 50 years, see e.g. a review by Issi (1979). Recently, with the development of reliable and convenient cooling provided by dilution refrigerators, the measurements have been extended to temperatures below 1 K (Pratt and Uher 1978). The data provided new and important information on the scattering mechanisms of phonons and the relative contributions of free carriers and lattice waves to the total thermal conductivity.

Owing to the low intrinsic carrier concentration, dopant species may be introduced into a Bi matrix, where they not only act as strong scattering centres for both the charge carriers and phonons, but also drastically modify the Fermi surface. Typical dopants are Sn and Te, the former acting as an acceptor, the latter donating free electrons. For an up-to-date review of the effect of doping on Bi see e.g. Heremans and Hansen (1983).

In his recent studies of Sn-doped Bi polycrystals, Uher (1979) has extended the measurements of the resistivity and thermopower down to 50 mK and the data revealed several novel and unexpected features, in particular the onset of a superconducting transition below 60 mK and an enormous phonon drag contribution to the thermopower near 4 K. High thermopower values were also measured on Sn-doped Bi single crystals by Boxus *et al* (1979). Along these lines, it was found interesting to carry out detailed thermal conductivity measurements on a series of Sn-doped bismuth samples below 1 K.

‖ Present address: Physics Department, General Motors Research Laboratories, Warren, MI 48090, USA.

0022-3719/85/153001 + 10 $02.25  

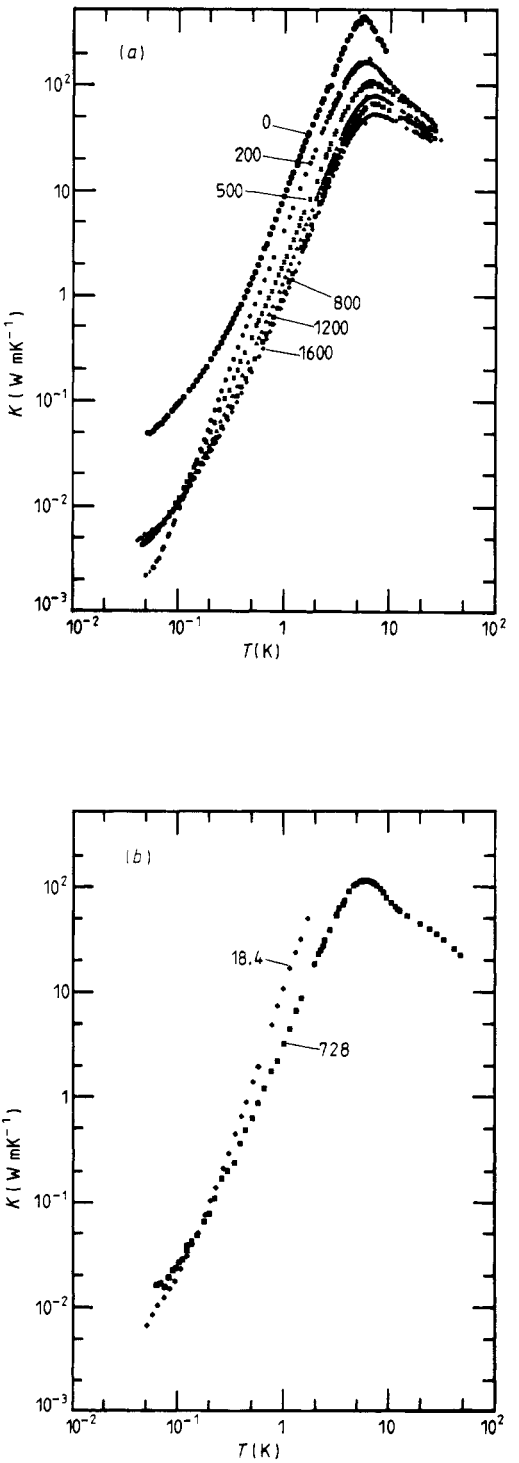


**Figure 1.** Experimental values for the temperature dependence of the thermal conductivity of polycrystalline (*a*) and single crystal (*b*) samples of bismuth. The Sn concentrations, in atomic ppm, identify the various curves.

Our primary aim was to find out how the thermal conductivity is affected by doping. In this paper we report our findings and also attempt to interpret them quantitatively.

## 2. Experimental

The samples used in the measurements come from two different sources: The polycrystalline samples (grain size 0.2 to 0.3 mm) are identical to those used by Uher and Opsal (1978) and Uher (1979) in the investigations of the resistivity and thermopower; the single crystals were prepared and characterised by Noothoven van Goor (1971) and some of their transport properties were studied by Boxus *et al* (1979, 1983) and by Heremans and Hansen (1983). Doping levels and other relevant parameters are given in table 1. The sample identification given in that table is common to all the previous work published on those samples.

**Table 1.** The low-temperature electronic thermal conductivity of Sn-doped bismuth. The values for the electrical resistivity are those reported at 4.2 K by Noothoven van Goor (1971) for the single crystals, and by Uher (1979) for the polycrystals. The single crystals have their long axis oriented along the bisectrix direction.

| Sample | Structure | Sn (at. %) | RRR | $\rho_0$(4.2 K) ($10^{-7}$ ohm m) | $K_E/T$ (W m$^{-1}$ K$^{-2}$) | $4K_E/K$ at 0.08 K (%) |
|---|---|---|---|---|---|---|
| Bi 72 | single crystal | 0.00184 | 5.43 | 2.08 | 0.117 | 68 |
| Bi J728 | single crystal | 0.0728 | 10.1 | 2.26 | 0.108 | 43 |
| Bi | polycrystal | 0 | 40 | 0.3 | 0.813 | 90 |
| Bi +0.02 | polycrystal | 0.02 | 1.48 | 1.2 | 0.0203 | 32 |
| Bi +0.05 | polycrystal | 0.05 | 6.40 | 3.79 | 0.0644 | 61 |
| Bi +0.08 | polycrystal | 0.08 | 7.05 | 3.67 | 0.0665 | 68 |
| Bi +0.12 | polycrystal | 0.12 | 8.56 | 3.40 | 0.0718 | 74 |
| Bi +0.16 | polycrystal | 0.16 | 9.29 | 3.19 | 0.0765 | 78 |

Measurements below 4 K were made in dilution refrigerators at the University of Michigan (polycrystalline samples) and at Grenoble (single crystals). In the former case, the temperature gradient was determined with the aid of two germanium sensors which were calibrated against the superconducting fixed-point standards as well as against a CMN thermometer. In the latter case, measurements were limited to below 1 K and carbon thermometers were calibrated against a CMN thermometer. The data at higher temperatures were obtained in a conventional helium-4 cryostat. Small metal film resistors served as heaters in most of the measurements. The experimental data are shown in figure 1 and it is clear that the overlap between the two temperature ranges is satisfactory.

## 3. Theoretical models

In general, the low-temperature thermal conductivity of solids consists of two independent terms, the conductivity associated with the transport of charge carriers, $K_E$, and the conductivity arising from lattice $K_L$. The total thermal conductivity is then

$$K = K_E + K_L. \tag{1}$$

We shall discuss each contribution in turn.

### 3.1. Electronic thermal conductivity

While most of the heat is carried by phonons in pure and doped bismuth between 2 and 50 K, this is not necessarily so at very low temperatures, where the electronic thermal conductivity diminishes more slowly than the lattice conductivity. We attribute the bending of the $K(T)$ curves observed at the lowest temperatures (see figure 1) to just this effect. In this temperature range elastic impurity scattering dominates and we assume that the Wiedemann–Franz law is obeyed:

$$K_E = L_0 T/\rho_0 \tag{2}$$

where $L_0 = 2.44 \times 10^{-8}\ V^2\ K^{-2}$ is the free-electron Lorenz number, and $\rho_0$ is the residual value of the resistivity given in table 1. The values of $K_E/T$ as determined from equation (2) are also presented in table 1. By subtracting the electronic contribution from the total thermal conductivity, one obtains the lattice thermal conductivity which is shown in figures 2(*a*) and (*b*) for the case of polycrystalline and single-crystal samples, respectively. It may be seen that the upward bending near 0.1 K has now nearly disappeared as expected. The fraction of the thermal conduction due to the electron transport, $K_E/K$, at 0.08 K (see table 1) shows that $K_E$ is often the most important contribution at low temperatures. The value of the lattice thermal conductivity, $K_L$, which is then obtained as a difference between two large numbers, shows a progressively increasing uncertainty as the temperature decreases.

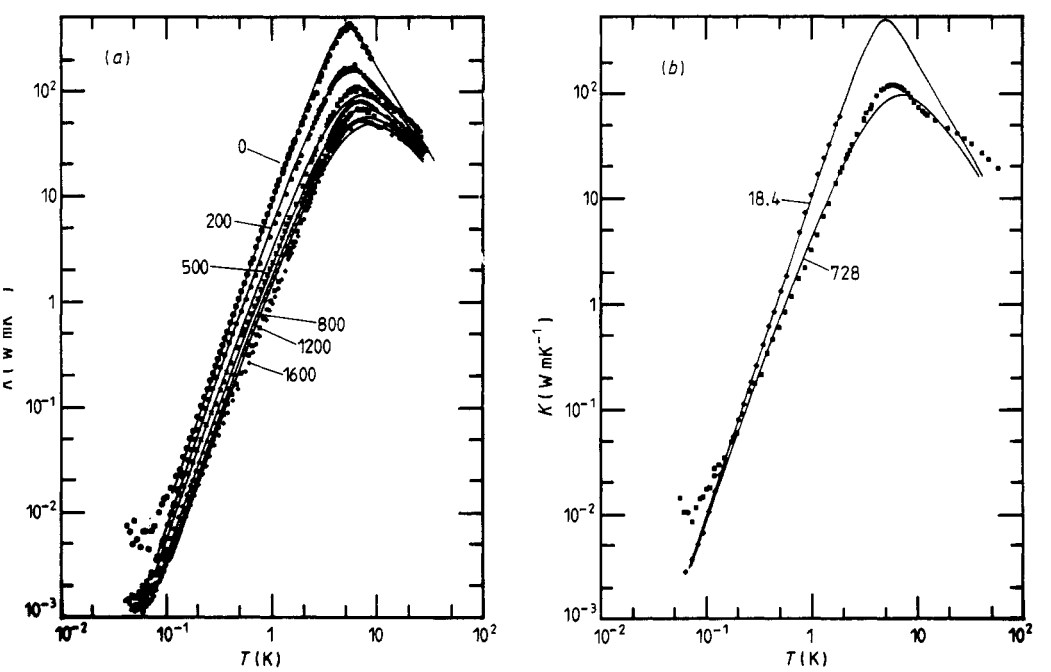


**Figure 2.** The temperature dependence of the lattice thermal conductivity of the polycrystalline (*a*) and single crystal (*b*) samples of Bi. The points represent the 'experimental' values for $K_L$ obtained by subtracting the electronic thermal conductivity, $K_E$ (table 1), from the experimental total thermal conductivity given in figure 1. The curves are the results of the model calculations using Callaway's theory, equation (13), and the parameter values listed in table 2.

### *3.2. Lattice thermal conductivity*

It is reasonable to assume that the main influence of the doping impurity is to scatter the phonons; we shall neglect any influence it could have on the phonon spectrum itself, or on phonon–phonon interactions. Sosnowski (1981) reported that Sb doping does not much effect the acoustic phonon spectrum of bismuth. We also argue that due to the low free carrier density ($<10^{-3}$ carriers per atom) even in the most highly doped samples, the phonon–carrier scattering is unlikely to play a significant role in comparison with phonon–impurity scattering. This particular point has recently been discussed by Boxus *et al* (1983). In calculating the value of $K_L$ we shall follow the method outlined by Berman (1976) and consider the mechanisms which lead to phonon scattering.

*3.2.1. Large-scale defect scattering.* The relaxation frequency for phonon scattering on defects of much larger size than the phonon wavelength such as e.g. crystal boundaries is given by

$$\tau_L^{-1} = v/L \tag{3}$$

where $v$ is the phonon velocity and $L$ is the average distance between such defects. In the pure polycrystalline sample $L$ ought to be equal to the average size of the crystallites, provided the boundaries reflect the phonons diffusely. If low-energy acoustic phonons dominate the thermal transport, as is usually the case, $\tau_L$ is independent of the phonon frequency $\omega$.

*3.2.2. Point defect scattering.* When the size of the impurity is small compared with the phonon wavelength, one uses the notion of 'point defects'. This is the case for isotopes, or, within certain limits, for substitutional impurity atoms. The latter are, indeed, usually surrounded by a strain field which renders the treatment of their influence on the thermal conductivity more delicate. As has already been suggested (Boxus *et al* 1983), this may be an important scattering mechanism in doped bismuth. For a phonon of frequency $\omega$, the scattering rate on point defects is

$$\tau_p^{-1} = Px^4T^4 \tag{4}$$

where

$$x = \hbar\omega/kT. \tag{5}$$

If we neglect the influence of strain fields around the point defect, the parameter $P$ becomes

$$P = (k/\hbar)^4(\Delta M/M)^2 c_p a^3/4\pi v^3 \tag{6}$$

(see Klemens 1955, 1969). In this equation, $c_p$ is the atomic concentration of the point defects; $a^3$ is the atomic volume which for bismuth is $3.5 \times 10^{-29}$ m$^3$; $(\Delta M/M)$ is the relative difference between the atomic mass of the substitutional atoms and the atomic mass of the host atoms. For tin impurity in bismuth $\Delta M/M = 0.432$.

*3.2.3. Dislocations.* Another type of defect which can scatter phonons is dislocations which give a relaxation frequency (Berman 1976)

$$\tau_D^{-1} = DxT \tag{7}$$

where the parameter $D$ is linearly related to the density of dislocations, $N_d$ (Klemens 1955, 1969)

$$D = 0.61(k/\hbar)N_d b^2 \gamma^2. \tag{8}$$

$b$ is the Burgers vector, which is taken equal to the interatomic distance of 4.5 Å, and $\gamma$ is the Grüneisen parameter equal to 1.9 at very low temperature (White 1972).

*3.2.4. Phonon–phonon processes.* In discussing the intrinsic phonon–phonon scattering, we must distinguish between Umklapp and Normal processes. *Umklapp* processes lead to a phonon–phonon interaction frequency described by

$$\tau_U^{-1} = Ux^2T^2 \exp(-U_e\theta_D/T) \tag{9}$$

where $\theta_D$ is the Debye temperature (120 K) and $U$ and $U_e$ are adjustable parameters. *Normal* processes involve the interaction between two phonons of small enough momentum so that the resultant phonon remains within the Brillouin zone. According to Herring (1954a, b), the relaxation frequency for subthermal phonons in a rhombohedral crystal is described by $\tau^{-1} = Aq^3T^2$, where $q$ is the phonon momentum and $A$ is a constant. For bismuth, Issi *et al* (1976) found a value of $39 \times 10^{-23}\ \mathrm{m^3\ s^{-1}\ K^{-2}}$. In our temperature range $T < \theta_D/10$, and we assume that this relaxation rate describes the normal phonon processes. Hence,

$$\tau_N^{-1} = Nx^3T^5 \tag{10}$$

where $N = 88.1\ \mathrm{s^{-1}\ K^{-5}}$.

*3.2.5. The Callaway model.* Since large-scale defect, point defect and dislocation scattering as well as phonon–phonon Umklapp processes are dissipative, the scattering rate for the resistive phonon processes is

$$\tau_R^{-1} = \tau_L^{-1} + \tau_p^{-1} + \tau_D^{-1} + \tau_U^{-1}. \tag{11}$$

The Normal processes favour the generation of higher-momentum phonons, but through the interaction in which the total momentum is preserved. However, these higher-momentum phonons in turn are more liable to undergo resistive processes. Callaway (1959) developed a treatment that we shall follow here. It is based on the definition of the relaxation time $\tau_C$ given by

$$\tau_C^{-1} = \tau_R^{-1} + \tau_N^{-1}. \tag{12}$$

Callaway's expression for the thermal conductivity may then be written as:

$$K_L = K_1 + K_2 \tag{13a}$$

where

$$K_1 = \frac{k}{2\pi^2 v}\left(\frac{k}{\hbar}\right)^3 T^3 \int_0^{\theta/T} \tau_C f(x)\,\mathrm{d}x \tag{13b}$$

and

$$K_2 = \frac{k}{2\pi^2 v}\left(\frac{k}{\hbar}\right)^3 T^3 \left(\int_0^{\theta/T} \frac{\tau_C}{\tau_N} f(x)\,\mathrm{d}x\right)^2 \Big/ \left(\int_0^{\theta/T} \frac{\tau_C}{\tau_N \tau_R} f(x)\,\mathrm{d}x\right) \tag{13c}$$

in which

$$f(x) = x^4 e^x/(e^x - 1)^2. \tag{13d}$$

Sound velocities for all phonon modes along all high-symmetry propagation directions have been measured by Eckstein *et al* (1960). In equation (13), we use an average over the three modes given by

$$v = \left[\frac{1}{3}\left(\frac{1}{v_L^3} + \frac{1}{v_{T1}^3} + \frac{1}{v_{T2}^3}\right)\right]^{-1/3} \tag{14}$$

and also take the cube average over the propagation directions. The sound velocity at 4.2 K is 1300 $ms^{-1}$. It is to be noted that the slower transverse modes dominate in the average.†

### *3.3. The fitting procedure*

Computer programs were written to fit the lattice thermal conductivity to Callaway's expression, equation (13), with various unknown parameters $L$, $P$, $U$ or $U_e$ defined in equations (3)–(11). All experimental curves show that the thermal conductivity increases with temperature following a $T^n$ law, where $n$ has a value between 2 and 3. There is a maximum in conductivity at a temperature between 3 and 5 K. In the low-temperature regime, it is mostly large-scale impurities and dislocations that dominate the scattering. Near the maximum, point-defect scattering is important. The decrease at high temperatures is mainly due to the influence of the Umklapp phonon–phonon processes, which are an intrinsic feature of the bismuth conduction.

Because the various scattering mechanisms influence the thermal conductivity in different temperature regimes, we can avoid the use of a cumbersome and blind computer routine operating on all parameters simultaneously over the whole temperature range. We shall work in three steps:

(i) The low-temperature lattice conductivity well below the maximum will be fitted by adapting $L$ and $D$ (large-scale impurity and dislocation scattering).

(ii) The lattice thermal conductivity of the pure samples will then be used to yield values for the Umklapp parameters $U$ and $U_e$, which are assumed to be independent of the doping density. For this purpose we use the results of figure 2 for our pure polycrystalline Bi and the data of Kuznetsov *et al* (1969) on single crystals.

(iii) Finally, we use the fitting routine to find the optimum value of the point defect parameter $P$ for all samples.

To determine the value of $L$ and $D$, we approximate the Callaway expression (13) in the low-temperature regime by (Berman and Brock 1965):

$$\frac{K_L}{T^3} = \frac{2\pi^2}{15}\frac{k^4}{\hbar^3}\frac{L}{v^2}\left(1 - 4.8\frac{L}{v}DT\right). \tag{15}$$

From equation (15), a linear relation between $K_L/T^3$ and $T$ at low temperatures may be assumed symptomatic of dislocation scattering. Unfortunately, the results of Kuznetsov *et al* on a bisectrix sample, do not extend to sufficiently low temperatures to reveal such a linear relation. We can only infer that $K_L/T^3$ probably saturates at a value of 47 $W\,m^{-1}\,K^{-4}$ from which we deduce the value of $L$ reported in table 2. The data for sample Bi 72 fall on a horizontal line which suggests the absence of dislocation scattering

† McDonald and Anderson (1983) use a quadratic average over the sound velocities in a formula $K = cvl$ where $c$ is the specific heat and $l$ the phonon mean free path. Numerically, there is no significant difference between velocities obtained through quadratic or cubic averages.

**Table 2.** Values of the parameters used in fitting the thermal conductivity data. The values reported for $P$ are three times those obtained by equation (6).

| Sample name | $c_p$ (ppm) | $L$ (mm) | $D$ ($10^6\,s^{-1}\,K^{-1}$) | $N_d$ ($10^{12}\,m^{-2}$) | $P$ ($K^{-4}\,s^{-1}$) |
|---|---|---|---|---|---|
| Bi (Kuznetsov) | | 1.92 | | | |
| Bi 72 | 18.4 | 0.39 | <0.01 | <0.02 | 3.9 |
| Bi J728 | 728 | 0.45 | 1 ± 0.5 | 2 ± 1 | 152 |
| Bi | 0 | 0.39 | 0.091 | 0.16 | 0 |
| Bi +0.02 | 200 | 0.31 | 0.37 | 0.63 | 42 |
| Bi +0.05 | 500 | 0.25 | 1.1 | 1.9 | 105 |
| Bi +0.08 | 800 | 0.17 | 1.6 | 2.7 | 168 |
| Bi +0.12 | 1200 | 0.14 | 2.15 | 3.7 | 251 |
| Bi +0.16 | 1600 | 0.12 | 2.5 | 4.3 | 335 |

The fitted parameters are determined within 10%, except for Bi J728, where $D$ and $N_d$ are within 50% as quoted.

and yields a value of $L$. Pure polycrystalline bismuth obeys equation (15) closely. The linear variation is apparent in doped polycrystals only at the lowest temperatures and the fit deteriorates progressively with increasing impurity concentration. However, in order to reproduce the smooth power law with an exponent between 2 and 3 displayed by the experimental curves in figure 2, the inclusion of a non-zero value of the parameter $D$ is essential. The values of $D$ given in table 2 were obtained by fitting equation (15) below 0.5 K. Exactly the same procedure was used for the single crystal Bi J728.

Having determined the parameters $L$ and $D$ using equation (15), we proceed to solve the full Callaway model, equation (13). We define an error function

$$\mathrm{Err} = \sum_{\substack{\text{all experimental}\\ \text{points}}} \left(1 - \frac{K_{\text{calculated}}}{K_{\text{experimental}}}\right)^2 \tag{16}$$

which is to be minimised by an appropriate choice of variables $U$, $U_e$ and $P$. We first apply this procedure to the data for pure Bi, where $U$ and $U_e$ are the only relevant parameters ($P$ is taken to be zero as Bi is monoisotopic). The results are $4000\,s^{-1}\,K^{-2}$ and 0.12 for $U$ and $U_e$ respectively. These values of the Umklapp parameters are used in the subsequent analysis of the doped samples for which $P$ is non-zero.

It is worth noting that if we ascribe a 10% higher value for $U$ and $U_e$ it yields, according to the sample considered, a 1 to 2% change in the error function (equation (16)). This means that $U$ and $U_e$ cannot be estimated to better than 10% and is due to the presence of the small hump above the maximum in the experimental data above 10 K which is not accounted for in equation (13).

As regards the sensitivity of the coefficients to the constrained parameters, there is no influence of $L$ or $D$ on $U$, $U_e$ or $P$, since they come into play at quite different temperature ranges. However, this is not the case for the mutual effect of $U$, $U_e$ and $P$: a 10% change in $U$ or $U_e$ results in a 10% shift in the optimal value of $P$ to fit the curves.

## 4. Discussion

The results of the calculations using the parameters collected in table 2 are shown in

figure 2 from which the quality of the fits can be appreciated. Overall these fits are quite reasonable and the agreement is particularly good for samples of low impurity content.

The values of the point-defect parameter $P$ may be estimated from equation (6) if we take the density of scattering centres to be the density of impurity atoms in the crystal, $c_p$. The latter quantity is reported in table 2. The optimised values of $P$ are about a factor of three larger than those calculated directly from equation (6). Henceforth, the value of $P$ adopted is the calculated value multiplied by three. This discrepancy between the calculated and fitted values of $P$ is not unusual (Klemens 1955) and may be due to the strain fields surrounding each impurity atom. Indeed, the dissimilarity of Bi and Sn atoms gives rise not only to the electronic doping effect but also to a considerable distortion of the bismuth lattice in the neighbourhood of the substitutional impurity. We note that the curve for the highly doped single-crystal J728 cannot be well described by the simple model used here, especially near 10 K where there is a small depression. Such a dip could be related to resonant phonon scattering due to a pseudo-localised mode introduced by the Sn impurity. Such phenomena have been observed in doped alkali halides (see for example Baumann and Pohl 1967). There is also a discrepancy between calculations and experiment near 1 K, which is also present for the most highly doped polycrystalline samples. The experimental values are lower than the calculated ones, which suggests the existence of an additional scattering mechanism. In this context, we mention that clusters of metallic tin have been detected in these samples (Uher 1979, Heremans *et al* 1979), and that they could be a source of phonon scattering, as are, for instance, $MgF_2$ precipitates in LiF (Neumaier 1969). Supporting this view is the fact that the values of $L$ obtained for the doped single crystals (table 2) are much smaller than the mean diameter of the samples (2.7 mm for Bi 72, 4.5 mm for Bi J728), while for pure bismuth single crystals the low-temperature thermal conductivity is actually limited by size-effects (Boxus *et al* 1981). In the pure and lightly doped polycrystals $L$ is also comparable with the size of the crystallites, 0.2 to 0.3 mm (Uher 1979). However, in the highly doped polycrystals $L$ is lowered to about $\frac{1}{2}$ or $\frac{1}{3}$ of this value.

Finally, we have estimated the density of dislocations $N_d$ for each sample, using equation (8) and the fitted values of $D$ which are given in table 2. It is well known that values of $N_d$ obtained in that way are systematically too large, and also that phonon scattering by vibrating dislocations could play a role (Berman 1976). However, the evolution of $N_d$ with doping is significant: $N_d$ clearly increases with Sn content, and the value for the single crystal Bi J728 is close to that obtained for polycrystals of equivalent tin concentration. We suggest that these larger values of $N_d$ could also be indicative of the presence of tin clusters in the highly doped samples.

## 5. Conclusion

We have extended the temperature range for the thermal conductivity studies on tin-doped bismuth down to 50 mK. Bismuth is a particularly suitable system to study the effect of doping because its intrinsic properties are well known and owing to its very low intrinsic carrier density, a substitutional impurity such as Sn affects not only phonon transport but also drastically alters the free carrier population. We have shown that the electronic thermal conductivity actually dominates the transport of heat at the lowest temperatures. We have analysed the lattice thermal conductivity using the Callaway's model in conjunction with the point-defect and boundary scattering and the agreement with the experiment is satisfactory in most cases. We do, however, find a discrepancy

between the experimental and theoretical thermal conductivities in the most heavily doped samples. The discrepancy could be reconciled by invoking an additional scattering mechanism that we speculate might be associated with the tendency of Sn particles to form clusters in the Bi matrix.

## Acknowledgments

We gratefully acknowledge the Nato travel grant No RG533/82 between the University of Louvain and the University of Michigan which was instrumental in setting up the collaborative effort between two of the groups. Part of the project was supported by NSF Low Temperatures Grant DMR-8304356.

## References

Baumann F C and Pohl R O 1967 *Phys. Rev.* **163** 843
Berman R 1976 *Thermal Conduction in Solids* (Oxford: Clarendon)
Berman R and Brock J C F 1965 *Proc. R. Soc.* A **289** 46
Boxus J, Heremans J, Michenaud J-P and Issi J-P 1979 *J. Phys. F: Met. Phys.* **9** 2387–98
Boxus J, Issi J-P, Michenaud J-P and Heremans J 1983 *Proc. 16th Int. Conf. on Thermal Conductivity* ed. D C Larsen (New York: Plenum) pp 47–58
Boxus J, Uher C, Heremans J and Issi J-P 1981 *Phys. Rev.* B **23** 449
Callaway J 1959 *Phys. Rev.* **113** 1046
Eckstein Y, Lawson A W and Renecker D H 1960 *J. Appl. Phys.* **31** 1534
Heremans J, Boxus J and Issi J-P 1979 *Phys. Rev.* B **19** 3476–87
Heremans J and Hansen O P 1983 *J. Phys. C: Solid State Phys.* **16** 4623–36
Herring C 1954a *Phys. Rev.* **95** 954
—— 1954b *Phys. Rev.* **96** 1163
Issi J-P 1979 *Aust. J. Phys.* **32** 585
Issi J-P, Michenaud J-P and Heremans J 1976 *Proc. 14th Int. Conf. on Thermal Conductivity* ed. P G Klemens and T K Chu (New York: Plenum) pp 127–33
Klemens P G 1955 *Proc. Phys. Soc.* A **68** 1113
—— 1969 *Thermal Conductivity* vol. 1, ed. R P Tye (London: Academic) ch 1, p 1
Kuznetsov M E, Oskotskii V S, Pol'shin V I and Shalyt S S 1969 *Zh. Eksp. Teor. Fiz.* **57** 1112–7
—— 1970 *Sov. Phys.-JETP* **30** 607–9
McDonald W M and Anderson A C 1983 *Proc. 17th Int. Conf. on Thermal Conductivity* ed. J G Hust (New York: Plenum) p 185
Neumaier K 1969 *J. Low Temp. Phys.* **1** 77
Noothoven van Goor J M 1971 *Philips Res. Rep.* Suppl. **4** 1
Pratt W P and Uher C 1978 *Phys. Lett.* **68**A 74–6
Sosnowski L 1981 *Phys. Status Solidi* b **104** 97
Uher C 1979 *J. Phys. F: Met. Phys.* **9** 2399–410
Uher C and Opsal J L 1978 *Phys. Rev. Lett.* **40** 1518–21
White G K 1972 *J. Phys. C: Solid State Phys.* **5** 2731